*Turkish Journal of Computer and Mathematics Education Vol.12 No.12 (2021), 263-273*

*Research Article*

# Steel Surface Defect Detection Using Glcm, Gabor Wavelet, Hog, And Random Forest Classifier

**Chetan Vasant Chaudhari[1], Dr. Ravindra Kumar Gupta[2], Sapana A. Feagade[3]**

[1]Research Scholar, Computer Science & EngineeringIES IPS Academy, IndoreMP, India.
[2]Computer Science EngineeringRKDF Institute of Science & Technology,Bhopal, India.
[3]Computer Science & Engineering SKCLNCT, Indore MP, India.
[1]chaudharichetanv@gmail.com, [2]ravindra_p84@rediffmail.com, [3]sapana.fegade4@gmail.com

**Article History**: Received: 11 January 2021; Revised: 12 February 2021; Accepted: 27 March 2021; Published online: 23 May 2021

**Abstract–**In the current context of market opening, quality control is essential in the field of steel production where quality is combined with the reduction in manufacturing costs. This control can be described as a set of systems deployed to verify and maintain the desired level of quality. In the manufacturing processes of steel products, great importance is allocated to the surface condition and the possibilities of its inspection, production in progress. Simple visual inspection is unable to follow the product which is generally in motion, and even with a reduced speed of the process, the inspection of the surface can only be carried out as a sampling, which is not exhaustive. Inspection at the end of the process, for its part, could not be the ideal solution, since it will only allow the history of the process to be traced, and information on its trends. Therefore, defects in the final product, which are not detected and corrected, lead to the downgrading of products and incur additional costs.Automatic detection and recognition of surface faults in the metallurgical industry are objectives for which new technologies are being implemented, to obtain greater quality control and competitive advantages in production. To this end, a machine learning-based system is presented in this paper for the inspection of steel surface defects using various feature extraction techniques; Gray-Level Co-Occurrence Matrix (GLCM), Gabor Wavelet, and Histogram of Oriented Gradients (HOG). The classification of extracted features is accomplished by Random Forest Classifier.

**Keywords –** Gabor Wavelet, GLCM, HOG, Random Forest Classifier.

## 1. Introduction

The evolution of civilizations and techniques is closely linked to the use of materials such as iron and steel. The latter is in fact at the origin of industrial revolutions and have been at the heart of great discoveries that have marked the development of humanity.

Today, steel production is one of the indicators of a country's wealth. Significant quantities of steel products are produced annually, and there is not one area of activity where this material is not present. The automotive industry, public works, shipbuilding, industrial and household equipment, etc., are all steel-consuming sectors. This craze for steel products has boosted the development of manufacturing techniques for different grades and the creation of more and more steel factories to meet the needs of society [1]. Investments in this sector are so important that they are always accompanied by a rigorous policy of profitability while meeting the needs in terms of quantity and quality [2].

In the recent past, the inspection of steel products, which has always been a necessity, involved additional tasks dedicated to measuring certain properties of the product being finished, or even going to the laboratory to check other parameters. However, the strong growth in demand for products for different uses and increasingly stringent quality requirements have imposed on manufacturers a frantic pace in the manufacture of products, and for which conventional and manual measurement and control methods provided, for many of them by experts, no longer seemed to represent the best solution [3].

This situation has led to further modernization in production lines, as well as to research and implementation of new means of process control and product quality control. Since then, the trend has been towards on-line supervision and at all levels of the production chain, and even on processes characterized by the aggressiveness of the environment (high temperature, presence of dust, water vapor, etc.). These new inspection methods have several advantages that boost production effort in this way. They ensure the very rapid or even premature identification of any problems, not only to allow intervention with a minimum of damage to material and installation but also to prevent a half-product with defects from automatically moving on to the following manufacturing operations. The detection, at this stage, of the defective product, avoids wasting time and energy in dealing with non-conformities at the end of the line [4].

The primary objective of surface inspection systems is the detection and classification of defects, taking into account the conformity requirements of a product for a given use. Based on machine vision, the first inspection

systems classified surface defects from a few gray level values, for example, a dark or very light spot could be taken as a hole. But the development of processing and acquisition means, in particular CCD sensor cameras, has made it possible to collect and analyze defect images for more efficient classification. Today these inspection systems based on artificial vision, machine vision, or sometimes called computer vision, or intelligent vision, continue to present the ideal solution for continuous control of product surfaces. They are more and more modernized and optimized, and are equipped, for this purpose, with intelligent algorithms which ensure their speed, precision, and reliability.

In the last decade, computer vision systems have established themselves as a fundamental piece for the quality control of different manufacturing systems [5]. In this field, the two most important applications of vision, in a broad sense, have been Automatic Visual Inspection and automatic assembly (Robotics).

### A. Vision System for Inspection

Broadly speaking, an industrial vision system is an application that combines hardware and software for acquiring and processing images and providing operational guidance for performing other tasks at the level of the body process or decision-making. This combination of tools has many advantages, which make the designed system an efficient solution for different applications. These are diverse and can relate, for example, to assistance in production such as robot guidance, control of assemblies of parts, or inspection for the identification of shapes and evaluation of dimensional conformity, or the detection and classification of faults.

The opportunity to have this advantageous solution, which is the vision system, has strengthened researchers and manufacturers in their choice, encouraged them to innovate in this field, and to multiply the objectives during its design. Among these objectives are those which are strategic such as:

- Improving quality and increasing productivity;
- Reducing costs and minimizing downtime;
- The optimization of product information management and process control with all aspects of traceability.

And other objectives, more technical, allow the system to be efficient in taking over different tasks. These objectives can be:

- The identification of faults with the minimum of classification errors;
- The ability to support real-time considerations;
- The possibilities of archiving faults, or even extending databases.

Typically a vision system is made up of one or more cameras placed facing the area to be inspected, acquisition module (s) for collecting images, lighting to enable the acquisition of images of the best possible quality, and calculator (s) for processing and analyzing information (Figure 1).

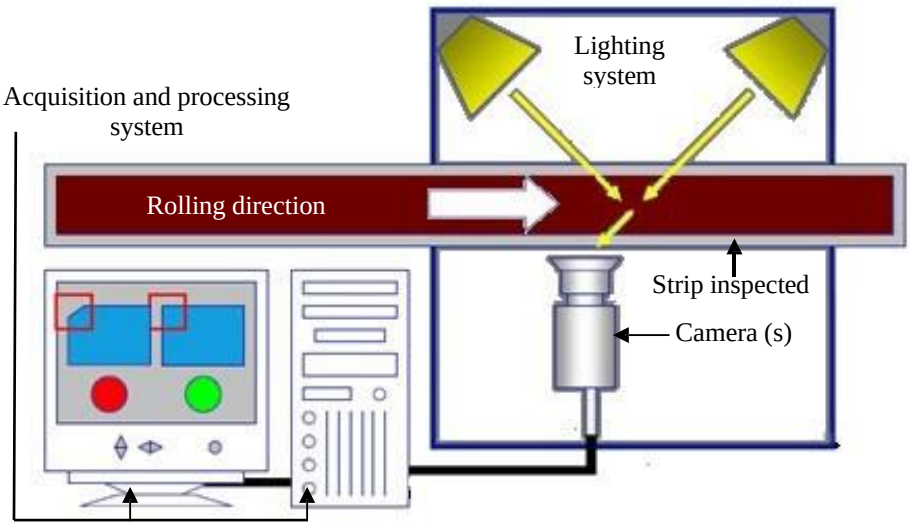


Figure 1: Simplified diagram of a vision system [6]

Beyond the advantages it represents in terms of collecting and processing information quickly, efficiently, and repeatedly with the required requirements (appropriate resolution, frame rate, measurement algorithms, etc.), the interest of a vision system lies, more, in the fact that it presents the ideal solution for operation in an industrial environment.

The type of material used in slitting lines is surface-treated steel; a remarkable optical characteristic of metals is that the electrons are excited by the energy of the absorbed photons decay, releasing that energy in re-emitted photons. Most of the absorbed light radiation is re-emitted in the form of visible light of the same wavelength. While in a glass the reflectivity is of the order of 0.05 (5%), the typical reflectivity of metal is between 0.90 and 0.95 (90 and 95%) although in this case, the reflectivity depends on the surface finish and for its determination, it is necessary taking experimental data to characterize the reflectivity of each type of coil. Generally, the coils have a surface treatment where the steel is covered by another material (zinc, tin, chromium, or organic films), mainly to increase its corrosion resistance. Some of these treatments are:

- Galvanized: Hot or cold rolled sheet coated on both sides with a layer of zinc, by immersion in a molten metal bath, to improve its corrosion resistance.
- Pre-painted: Steel product coated with paint in continuous lines, on one or both sides, with high resistance to corrosion and wide aesthetic possibilities, which make it ideal for application in the construction industries, household items, cold rooms, etc. It combines the high resistance of steel with the diversity of colors of paints.
- Cincalum - Galval: Steel products coated by the hot-dip process with an alloy of 55% aluminum and zinc, with high corrosion resistance. The Aluminum / Zinc coating offers a combination of barrier effect and galvanic protection that improves its performance in construction applications in both rural and industrial and marine environments.

### B. Previous Woks

Over the past decade, there has been a lot of research into computer vision technologies to detect surface defects that are not limited to metal surfaces. These techniques can primarily be divided into two groups, namely traditional image processing techniques and machine learning techniques that are based on characteristics of crafts or surface learning techniques. Traditional imaging techniques use primitive properties reflected by local anomalies to detect component defects, which can be categorized into construction methods, threshold methods, spectral methods, and model-based methods [7]. Construction methods include boundary operations [8], structure [9], template matching [10], and morphology [11]. Threshold methods comprise contrast adjustment threshold method [12], Otsu method [13], optimal threshold [14], watershed transform [15], and so on. The spectral methods usually include the wavelet transform [16], Gabor wavelet [17] and Fourier transform [18]. The low-rank matrix model [19] and Gaussian mixture entropy model [20] are model-based methods. Machine learning techniques typically involve two steps, namely feature extraction and model classification. By analyzing the properties of the input image, a feature vector is generated to describe the defect information, and then a feature vector is inserted into a pre-trained sorting model to determine if the input image is defective or not. These functions include the gray level co-occurrence matrix (GLCM) [21], local binary patterns (LBP) feature [22], histogram of oriented gradient (HOG) features [23], and so on [24]. Although these detection algorithms have produced better analytical results in various surface defect analyses, they cannot be applied directly to the metal surfaces mentioned above. Traditional image processing techniques often require multiple thresholds that overcome various disadvantages of an algorithm that is very sensitive to lighting conditions and background color. When new problems arise, this threshold should be set, or even the algorithm may need to be revised. Also, the characteristics revealed by industrial or surface training methods are not sufficiently distinguishable for difficult situations. This method usually targets specific scenarios that lack adaptability and strength to the previous sensing environment.

The proposed approach in this paper uses GLCM, Gabor wavelet, and HOG techniques for feature extraction and Random forest classifier for the classification of extracted features in a steel surface defect detection model.

## 2. Proposed Methodology

The proposed system is developed in three stages: in the first one, image acquisition for which the defect to be detected; in the second, techniques of feature extraction are studied, and in the third, a classification system using random forest classifier for the steel surface defect detection system. Figure 2 shows the flow diagram for the proposed approach.

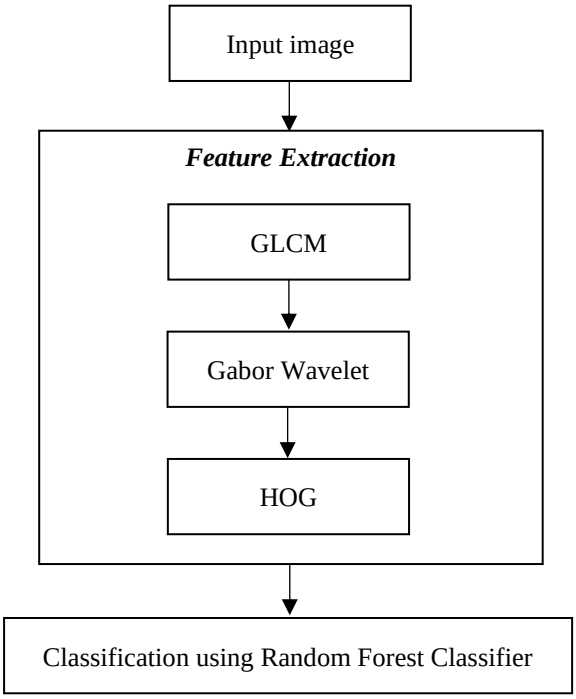


Figure 2: Flow diagram for proposed steel surface defect detection

**A. Image Acquisition**

This task, which is a critical step, because it has to reproduce an image and as faithfully as possible the observed scene to facilitate subsequent processing. The quality of the image, on the other hand, is based, among other key elements, on the environment and the conditions under which the acquisition is carried out. This paper uses the Kaggle steel defect detection dataset available at [25].

**B. Feature Extraction**

It aims to extract the features contained in the input image. These desired features are most often those which are independent, and must best characterize the image representing the product under inspection. It may be, for example, measurement of sizes or contours by the detection of edges, segmentation, and thresholding for the search for regions and other evaluation of the texture. The search for such characteristics of the image can make use of a multitude of statistical techniques, neural networks, etc. to arrive at a reliable descriptor of the acquired image. In this paper, three features extraction methods are used as follows:

**1. Gray Level Co-occurrence Matrix (GLCM)**

The elements of a co-occurrence matrix describe the frequency with which gray-level transitions occur in an image [26]. That is, an element in row $i$and column$j$ with a $p$-value in this matrix indicates that there were$p$ variations from gray-level$i$ to gray level$j$. Therefore, the number of rows and columns in this matrix is proportional to the amount of gray levels and does not depend on the dimensions of the image under analysis. For the calculation of this matrix, the spatial relationships between the pixels in which the analysis of the gray level variation will be made are defined.

The co-occurrence matrix is formally defined as follows: An image $I$is a function that associates a gray tone for each pixel, that is$I: D \rightarrow G$, where $D$is the domain of the image and$G = \{1,2, \dots, N_g\}$ is the set of gray levels. Let$S \subset D \times D$ be a set of ordered pairs of pixels.

$S$ is the set that defines which pairs of pixels will be considered in the analysis of the variation of gray levels. The co-occurrence matrix $P(i,j)$ is defined as:

$$P(i,j) = \#\{(u,v) \in S \mid I(u) = i \ \ and \ \ I(v) = j\} \quad (1)$$

After calculating the co-occurrence matrix, it is normalized by dividing each of its elements by the sum of the matrix:

$$p(i,j) = \frac{P(i,j)}{\sum_{i=1}^{N_g} \sum_{j=1}^{N_g} P(i,j)} \quad (2)$$

Haralick et al. [26] defined $S$certain angles and distances between pixels. For this, two additional parameters $d\theta$and are created, which respectively represent the distance between the two pixels and the angle that the line passing through these pixels makes with the horizontal. Most techniques that use the co-occurrence matrix assume four values for$\theta$: 0°, 45°, 90°, and 135°, as shown in Figure 3. For these spatial relationships between pixels, four co-matrices occurrences are constructed, one for each angle.

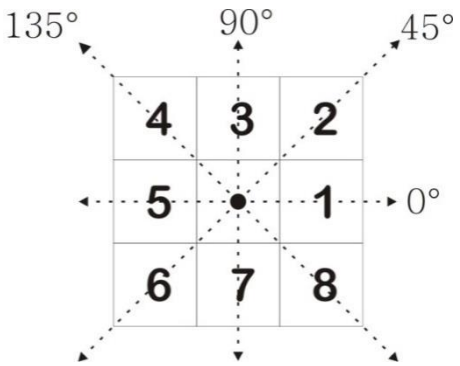


Figure 3: Angles used in the calculation of the gray level co-occurrence matrix [26]

**2. Gabor Wavelet**

Gabor wavelet features are measured for the proposed work. The directional decompositions for image analysis were probably initiated by Gaussian windowing in the 2D Fourier domain and continued 4D filters as well as the directional Gabor wavelets proposed by J. Daugman [27]. The use of Gabor's wavelets for the image is often linked to the consideration of the human visual system.

Gabor wavelets are constructed by isotropic Gaussian windowing of a complex plane wave of frequency $F$ in the direction $\theta$ [27, 30]:

$$\psi^{\theta}(x) = \frac{e^{-\|x\|^2/2}}{2\pi} e^{-j(x^T\omega_0)} \tag{3}$$

Where, $\omega_0 = F[\cos(\theta)\,;\sin(\theta)]^T$

The decomposition depends on the number of orientations $K$that one fixes, and that one can distribute evenly in$[0,\pi]$.

$$\theta \in \Theta = \left\{\frac{k\pi}{K}; 0 \le k \le K\right\} \tag{4}$$

We can then decompose any real 2D signal (x) by scalar product with the following atoms:

$$\left\{\psi_{j,u}^{\theta}(x) = 2^{-j}\psi^{\theta}\left(2^{-j}(x-u)\right)\right\}_{\theta\in\Theta, j\in\mathbb{Z}, u\in\mathbb{R}^2} \tag{5}$$

**3. Histogram of Oriented Gradients (HOG)**

A descriptor is used to transform an image into a space of characteristics, generally of high dimensionality, that allows highlighting some characteristic of the image so that it can be classified in definable sets, in this case, a defect on the steel surface and not a defect. The HOG descriptor is based on contour analysis by calculating gradients. The underlying idea presented by this descriptor is that the appearance and shape of an object in an image can be represented by the distribution of the orientations of the gradients.

The steps to obtain the descriptor are:

- The image is transformed into a grayscale.
- Gradients are calculated by partial derivatives in the horizontal and vertical directions$(I_x \text{ and } I_y)$. This is achieved by the respective convolutions with the mask $[-1\ 0\ 1]dx$for and $[-1\ 0\ 1]^T$for$dy$. Then the direction and angle of the gradient of each pixel are calculated. The result is then two matrices, one that represents the magnitudes of the gradient in each pixel of the original image and another matrix that contains the orientations of the same.
- The image is divided into descriptor blocks. These blocks of a preset size are arranged in such a way that they cover the entire image to be described with a predefined overlap between them.
- Each descriptor block is subdivided into cells.
- For each cell, a vector is calculated, where each element of it has the sum of the contributions of the gradients for a given direction or bins. The number of bins or elements in that vector can vary. Furthermore, the bins can be oriented in the 4 quadrants if magnitude and direction are considered for the contribution of the gradients, or only 2 quadrants if only magnitude and direction are considered.

- Normalization of the vectors is usually required due to variations in contrast and illumination.
- The bin vectors of the cells that form a block are concatenated with each other, resulting in a descriptor vector of the block.
- The vectors of each block are concatenated into a single image descriptor vector.

### C. Classification using Random Forest Classifier

A model is built from positive and negative examples, and through a learning algorithm, the most representative features of each training set are learned. For this purpose, the classification technique based on a random forest classifier is used.

Random forests were introduced by Breiman (2001) by the following very general definition [28]:

A Random Forest is a classifier comprising a set of elementary classifiers of the decision tree type, noted:

$$\{h(x, \Theta_k),\ k = 1, \dots L\} \tag{6}$$

Let $\left(\hat{h}(\Theta_1), \dots, \hat{h}(\Theta_q)\right)$ a collection of tree predictors, with $\Theta_1, \dots, \Theta_q$ random variables independent of $\mathcal{L}_n$ . The predictor of random forests $\hat{h}_{RF}$ is obtained is aggregating this collection of random trees as follows:

- $\hat{h}_{RF}(x) = \frac{1}{q}\sum_{l=1}^{q} \hat{h}(x, \Theta_l)$ Average of individual tree predictions in regression.
- $\hat{h}_{RF}(x) = \text{argmax}_{1 \le k \le K} \sum_{l=1}^{q} 1_{\hat{h}(x,\Theta_l)=k}$ A majority vote among individual prediction trees in classification.

The term random forest comes from the fact that individual predictors are, here, explicitly predictors per tree, and that each tree depends on an additional random variable (that is, in addition to $\mathcal{L}_n$ ).

The classification process followed by Random Forest consists of:

1. Assignment to a node if it is terminal, deciding whether a node will be labeled as a sheet or it will carry a test.
2. If the node is not terminal, then we have to select a test to assign it.
3. If the node is terminal, then we must give it a class.

The general algorithm for decision trees is as follows:

Input: sample S
Initialize the current tree to the empty tree;
The root designates the current node
Repeat
See if the current node is terminal
If the node is terminal then
Assign it a class
If not
Select a test and generate as many new child nodes as there are answers to this test
End if
Explore another node if there is one
Until a decision tree, A is obtained
Exit: decision tree A.

## 3. Simulation Results

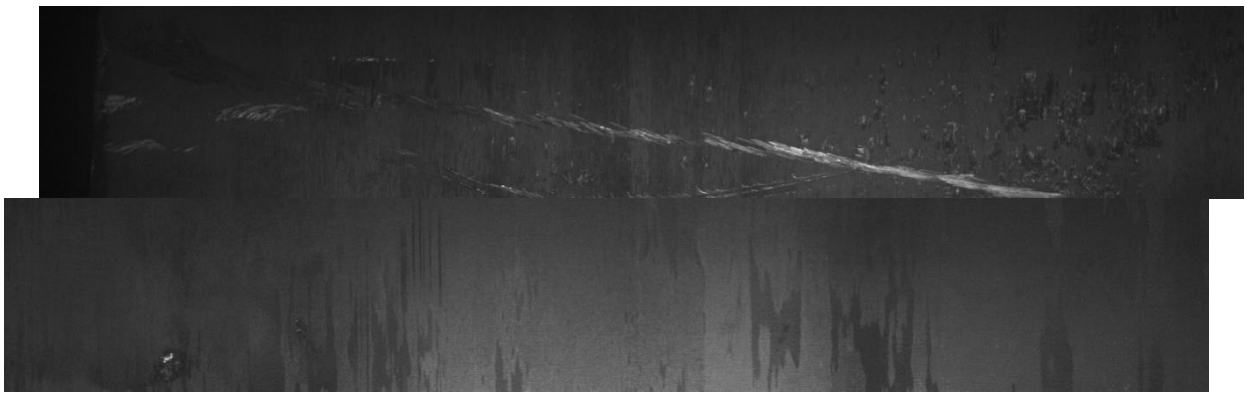

Figure 4: Sample images from the dataset [25]

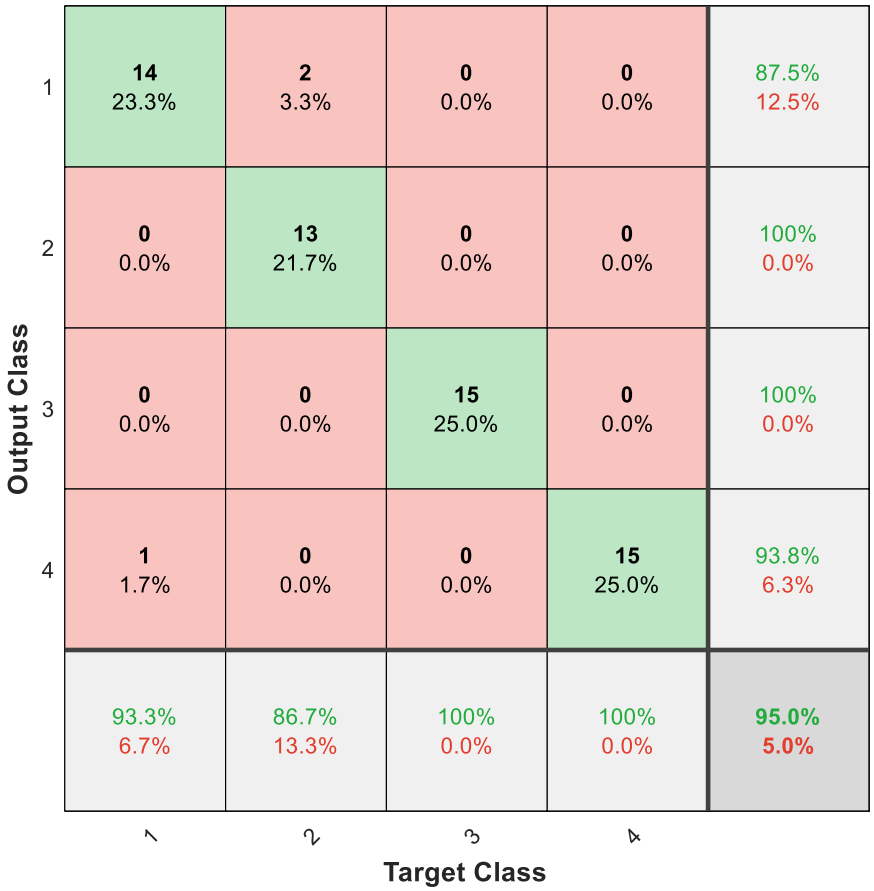


Figure 5: Confusion matrix plot for proposed steel surface defect detection

Figure 5 shows a confusion matrix plot for the Kaggle dataset. As per the dataset, it exhibits four classes for the four categories. The calculation for each class is given as follows:

Table 1: Result for GI dataset using SVM classifier

| Parameter | 1 | 2 | 3 | 4 |
|---|---|---|---|---|
| TP | 14 | 13 | 15 | 15 |
| FP | 1 | 2 | 0 | 0 |
| FN | 2 | 0 | 0 | 1 |
| TN | 43 | 45 | 45 | 44 |

**For '1':**

TP=14, TN=43, FP=1, FN=2

$$Accuracy = \frac{TP + TN}{TP + TN + FP + FN} = \frac{14 + 43}{14 + 43 + 1 + 2} = 95\%$$

$$Precision = \frac{TP}{TP + FP} = \frac{14}{14 + 1} = 93.33\%$$

$$Recall = \frac{TP}{TP + FN} = \frac{14}{14 + 2} = 87.5\%$$

$$MissRate = \frac{FN}{TP + FN} = \frac{2}{14 + 2} = 12.5\%$$

$$ErrorRate = \frac{FP + FN}{TP + TN + FP + FN} = \frac{1 + 2}{14 + 43 + 1 + 2} = 5\%$$

$$F - Score = \frac{2TP}{2TP + FP + FN} = \frac{2 \times 14}{2 \times 14 + 1 + 2} = 90.32\%$$

**For '2':**
TP=13, TN=45, FP=2, FN=0

$$Accuracy = \frac{TP + TN}{TP + TN + FP + FN} = \frac{13 + 45}{13 + 45 + 2 + 0} = 96.67\%$$
$$Precision = \frac{TP}{TP + FP} = \frac{13}{13 + 2} = 86.67\%$$
$$Recall = \frac{TP}{TP + FN} = \frac{13}{13 + 0} = 100\%$$
$$MissRate = \frac{FN}{TP + FN} = \frac{0}{13 + 0} = 0\%$$
$$ErrorRate = \frac{FP + FN}{TP + TN + FP + FN} = \frac{2 + 0}{13 + 45 + 2 + 0} = 3.33\%$$
$$F - Score = \frac{2TP}{2TP + FP + FN} = \frac{2 \times 13}{2 \times 13 + 2 + 0} = 92.85\%$$

**For '3':**
TP=15, TN=45, FP=0, FN=0

$$Accuracy = \frac{TP + TN}{TP + TN + FP + FN} = \frac{15 + 45}{15 + 45 + 0 + 0} = 100\%$$
$$Precision = \frac{TP}{TP + FP} = \frac{15}{15 + 0} = 100\%$$
$$Recall = \frac{TP}{TP + FN} = \frac{15}{15 + 0} = 100\%$$
$$MissRate = \frac{FN}{TP + FN} = \frac{0}{15 + 0} = 0\%$$
$$ErrorRate = \frac{FP + FN}{TP + TN + FP + FN} = \frac{0 + 0}{15 + 45 + 0 + 0} = 0\%$$
$$F - Score = \frac{2TP}{2TP + FP + FN} = \frac{2 \times 15}{2 \times 15 + 0 + 0} = 100\%$$

**For '4':**
TP=15, TN=44, FP=0, FN=1

$$Accuracy = \frac{TP + TN}{TP + TN + FP + FN} = \frac{15 + 44}{15 + 44 + 0 + 1} = 98.33\%$$
$$Precision = \frac{TP}{TP + FP} = \frac{15}{15 + 0} = 100\%$$
$$Recall = \frac{TP}{TP + FN} = \frac{15}{15 + 1} = 9.3.75\%$$
$$MissRate = \frac{FN}{TP + FN} = \frac{1}{15 + 1} = 6.25\%$$
$$ErrorRate = \frac{FP + FN}{TP + TN + FP + FN} = \frac{0 + 1}{15 + 44 + 0 + 1} = 1.67\%$$
$$F - Score = \frac{2TP}{2TP + FP + FN} = \frac{2 \times 15}{2 \times 15 + 0 + 1} = 96.77\%$$

## 4. Conclusion

The general performance of this architecture in both its learning and operational stages is improved when working with low-resolution images. The tests carried out have shown that the resolution is a significant parameter to reduce the processing time, the computational expense and thus improve the performance of the network.

Finally, the development of this system has a great impact on the metallurgical industry, since the automatic inspection of surface failures offers advantages such as the reduction of labor cost, the elimination of subjective judgments by the operators, and the creation of a base of data with the characteristics of the final product for analysis. The SVM classifier [29] achieves maximum accuracy of 95% with this research work.

**References**

1. Sun, X., Gu, J., Tang, S. and Li, J., 2018. Research progress of visual inspection technology of steel products—A review. Applied Sciences, 8(11), p.2195.
2. Kanno, R., Tsujii, M., Hanya, K., Matsuoka, K., Tominaga, T. and Ozaki, F., 2012. Steels, steel products, and steel structures sustaining the growth of society (infrastructure field). Nippon Steel Technical Report, 101, pp.57-67.
3. Fang, X., Luo, Q., Zhou, B., Li, C., and Tian, L., 2020. Research Progress of Automated Visual Surface Defect Detection for Industrial Metal Planar Materials. Sensors, 20(18), p.5136.
4. He, Y., Song, K., Meng, Q. and Yan, Y., 2019. An end-to-end steel surface defect detection approach via fusing multiple hierarchical features. IEEE Transactions on Instrumentation and Measurement, 69(4), pp.1493-1504.
5. Liu, Y., Geng, J., Su, Z., Zhang, W. and Li, J., 2019. Real-time classification of steel strip surface defects based on deep CNNs. In Proceedings of 2018 Chinese Intelligent Systems Conference (pp. 257-266). Springer, Singapore.
6. Neogi, N., Mohanta, D.K. and Dutta, P.K., 2014. Review of vision-based steel surface inspection systems. EURASIP Journal on Image and Video Processing, 2014(1), p.50.
7. Ren, R., Hung, T. and Tan, K.C., 2017. A generic deep-learning-based approach for automated surface inspection. IEEE transactions on cybernetics, 48(3), pp.929-940.
8. Tsanakas, J.A., Chrysostomou, D., Botsaris, P.N. and Gasteratos, A., 2015. Fault diagnosis of photovoltaic modules through image processing and Canny edge detection on-field thermographic measurements. International Journal of Sustainable Energy, 34(6), pp.351-372.
9. Tastimur, C., Yetis, H., Karaköse, M. and Akin, E., 2016. Rail defect detection and classification with real-time image processing technique. International Journal of Computer Science and Software Engineering, 5(12), p.283.
10. Jian, C., Gao, J. and Ao, Y., 2017. Automatic surface defect detection for mobile phone screen glass based on machine vision. Applied Soft Computing, 52, pp.348-358.
11. Rebhi, A., Abid, S. and Fnaiech, F., 2016, November. Fabric defect detection using local homogeneity and morphological image processing. In 2016 International Image Processing, Applications and Systems (IPAS) (pp. 1-5). IEEE.
12. Win, M., Bushroa, A.R., Hassan, M.A., Hilman, N.M. and Ide-Ektessabi, A., 2015. A contrast adjustment thresholding method for surface defect detection based on mesoscopy. IEEE Transactions on Industrial Informatics, 11(3), pp.642-649.
13. Yuan, X.C., Wu, L.S. and Peng, Q., 2015. An improved Otsu method using the weighted object variance for defect detection. Applied surface science, 349, pp.472-484.
14. Li, X., Gao, B., Woo, W.L., Tian, G.Y., Qiu, X. and Gu, L., 2016. Quantitative surface crack evaluation based on eddy current pulsed thermography. IEEE Sensors Journal, 17(2), pp.412-421.
15. Wang, L., Zhao, Y., Zhou, Y. and Hao, J., 2016. Calculation of flexible printed circuit boards (FPC) global and local defect detection based on computer vision. Circuit World.
16. Borwankar, R. and Ludwig, R., 2018. An optical surface inspection and automatic classification technique using the rotated wavelet transform. IEEE Transactions on Instrumentation and Measurement, 67(3), pp.690-697.
17. Hu, G.H., 2015. Automated defect detection in textured surfaces using optimal elliptical Gabor filters. Optik, 126(14), pp.1331-1340.
18. Bai, X., Fang, Y., Lin, W., Wang, L. and Ju, B.F., 2014. Saliency-based defect detection in industrial images by using phase spectrum. IEEE Transactions on Industrial Informatics, 10(4), pp.2135-2145.
19. Cen, Y.G., Zhao, R.Z., Cen, L.H., Cui, L.H., Miao, Z.J. and Wei, Z., 2015. Defect inspection for TFT-LCD images based on the low-rank matrix reconstruction. Neurocomputing, 149, pp.1206-1215.
20. Susan, S. and Sharma, M., 2017. Automatic texture defect detection using Gaussian mixture entropy modeling. Neurocomputing, 239, pp.232-237.
21. Chondronasios, A., Popov, I. and Jordanov, I., 2016. Feature selection for surface defect classification of extruded aluminum profiles. The International Journal of Advanced Manufacturing Technology, 83(1-4), pp.33-41.
22. Song, K. and Yan, Y., 2013. A noise-robust method based on completed local binary patterns for hot-rolled steel strip surface defects. Applied Surface Science, 285, pp.858-864.

23. Shumin, D., Zhoufeng, L. and Chunlei, L., 2011, July. AdaBoost learning for fabric defect detection based on HOG and SVM. In 2011 International conference on multimedia technology (pp. 2903-2906). IEEE.
24. Tao, X., Xu, D., Zhang, Z.T., Zhang, F., Liu, X.L. and Zhang, D.P., 2017. Weak scratch detection and defect classification methods for a large-aperture optical element. Optics Communications, 387, pp.390-400.
25. Severstal: Steel Defect Detection. Available online at: https://www.kaggle.com/c/severstal-steel-defect-detection/overview
26. Haralick, R.M., Shanmugam, K. and Dinstein, I.H., 1973. Textural features for image classification. IEEE Transactions on systems, man, and cybernetics, (6), pp.610-621.
27. Daugman, J.G., 1988. Complete discrete 2-D Gabor transforms by neural networks for image analysis and compression. IEEE Transactions on acoustics, speech, and signal processing, 36(7), pp.1169-1179.
28. Breiman, L., 2001. Random forests. Machine learning, 45(1), pp.5-32.
29. Raju, K., & RAO, Y. S. (2017). A NOVEL FUSION-BASED HYBRID APPROACH FOR FACE RECOGNITION SYSTEM. Journal of Theoretical & Applied Information Technology, 95(9).